

# Control of spin–spin exchange interactions in polynitroxides through inclusion within $\gamma$ -cyclodextrin†

Cite this: *RSC Advances*, 2013, 3, 427Mintu Porel,<sup>a</sup> M. Francesca Ottaviani,<sup>\*b</sup> Steffen Jockusch,<sup>c</sup> Nicholas J. Turro<sup>\*c</sup> and V. Ramamurthy<sup>\*a</sup>

Supramolecular interactions of polynitroxides with  $\gamma$ -cyclodextrin ( $\gamma$ -CD) were used to control intramolecular electron spin–spin exchange couplings in these stable radicals. In the absence of  $\gamma$ -CD, the binitroxide T2 and trinitroxide T3 showed strong spin–spin coupling as evidenced by the high exchange coupling constant of  $J = 120$  MHz for T2 in its EPR spectra. Host/guest complexes are formed upon addition of  $\gamma$ -CD to the polynitroxides where the nitroxide moiety interacts with the  $\gamma$ -CD cavity, which causes suppression of spin exchange. By variation of the host/guest ratio, the nature of a trinitroxide spin system can be tuned from a three-spin to a two-spin to a one-spin system. In addition to the host/guest ratio, the spin exchange coupling can also be tuned by temperature, which shifts the equilibrium between CD-encapsulated nitroxides and free nitroxides.

Received 18th September 2012,  
Accepted 2nd November 2012

DOI: 10.1039/c2ra22285j

[www.rsc.org/advances](http://www.rsc.org/advances)

## Introduction

Dynamic nuclear polarization (DNP), a method for enhancement of NMR signal intensities, has achieved great interest among chemists for its potential applications in magnetic resonance imaging (MRI).<sup>1</sup> Stable biradicals are of particular interest as coupling sources for DNP, because in this three-spin system (two electron spins and one nuclear spin) the efficiency of DNP can be controlled by tuning the coupling of the electron spins in the biradical.<sup>2</sup> Recently we have shown that spin–spin exchange coupling in a molecule substituted with two nitroxide groups can be tuned by supramolecular features using cage-like hosts, such as cucurbiturils and cyclodextrins.<sup>3</sup> We also showed that a series of polynitroxides (bi-, tri-, and tetranitroxides) are synthetically accessible from fluorinated cyano- and nitro- benzenes and that these polynitroxides showed strong spin–spin coupling.<sup>4</sup> These two findings, tuning the spin-interaction of a biradical and synthesis of new polyradicals, prompted us to examine the effect of supramolecular host–guest architectures to control spin–spin interactions in such polynitroxides. These effects and informations also open a wide range of possibilities for the use of these polynitroxides as spin probes in the analysis of complex systems.

Since in our earlier study binitroxide T2 and trinitroxide T3 (Scheme 1) showed strong spin–spin exchange we chose these compounds for the current investigation.<sup>4</sup>  $\gamma$ -Cyclodextrin ( $\gamma$ -CD, Scheme 1) was selected as a host as it had good solubility in MeOH–water (1 : 1) mixture in which the polynitroxide guests were also soluble.

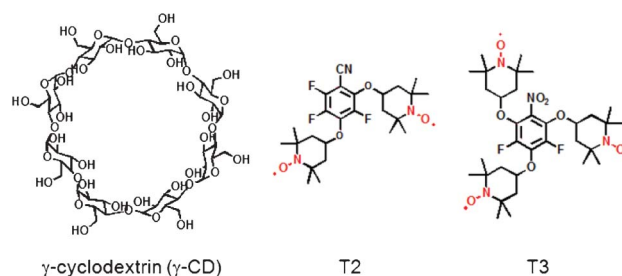
## Experimental

### Materials and methods

The biradical (T2) and triradical (T3) were synthesized using reported procedures.<sup>5</sup>  $\gamma$ -Cyclodextrin, a Sigma-Aldrich sample, was used as received.

### Preparation of host–guest complexes

A 20 mM chloroform stock solution of the guest and a 5 mM stock solution of  $\gamma$ -CD in water were prepared. The required amount of guest solution in chloroform was added in a vial



Scheme 1 Structures of the molecules used in this study.

<sup>a</sup>Department of Chemistry, University of Miami, Coral Gables, Florida, 33124, United States. E-mail: murthy1@miami.edu

<sup>b</sup>Department of Earth, Life and Environmental Sciences (DiSTeVA), University of Urbino, 61029 Urbino, Italy. E-mail: maria.ottaviani@uniurb.it

<sup>c</sup>Department of Chemistry, Columbia University, New York, 10027, United States. E-mail: njt3@columbia.edu

† Electronic Supplementary Information (ESI) available: EPR titration spectra, variable temperature EPR spectra, Arrhenius plots. See DOI: 10.1039/c2ra22285j

and the solvent was evaporated, to which calculated amounts of  $\gamma$ -CD solution, water and methanol were added to make the final ratio of water to methanol 1 : 1. The above solution was vigorously mixed with the help of a mechanical shaker for 15 h to ensure host-guest complexation.

### EPR study

EPR spectra were recorded on a Bruker EMX spectrometer at 9.5 GHz (X band) equipped with a Bruker ER4131VT variable temperature accessory. Spectrometer setting: power, 2 mW; amplitude modulation, 0.5 G; time constant, 164 ms; conversion time, 164 ms; field modulation, 100 KHz. Samples were taken in quartz (CFQ) EPR tubes (2 mm OD, 0.5 mm wall thickness, 10 cm height; Wilmad LabGlass) for the EPR experiments.

## Results and discussion

The experimental and simulated EPR spectra of T2 and T3 in MeOH-water (1 : 1) mixture at 293 K are provided in Fig. 1a and Fig. 2a, respectively. The simulation of the spectral line shape was performed by adding Lorentzian lines at the proper fields and widths. As previously described,<sup>4</sup> the spectra may be considered as constituted of the typical three-line spectrum of mononitroxide radical, superimposed onto multiplets of lines, which arise from strong spin-spin coupling between the nitroxide units in T2 and T3. The strong exchange interactions between the nitroxide units gives  $J \gg A_N$ , where  $J$  is the spin-spin exchange coupling and  $A_N$  is the coupling constant between the electron spin and the nitrogen nuclear spin. The three-line component is attributed to a conformation where the nitroxide radicals are far apart from each other, which does not allow spin-spin coupling ( $J = 0$ ).

After subtraction of the multiplet from the total spectrum, the three-line component attributed to uncoupled nitroxides was computed (Fig. 1a and Fig. 2a) using the well-established procedure of Freed and co-workers.<sup>6</sup> The most important parameters extracted from the computation are: (i) the coupling constant between electron and nitrogen nuclear spins  $\langle A_N \rangle = (A_{xx} + A_{yy} + A_{zz})/3$  which gives information about the environmental polarity of the nitroxides and (ii) the correlation time ( $\tau$ ) for the rotational diffusion motion of the

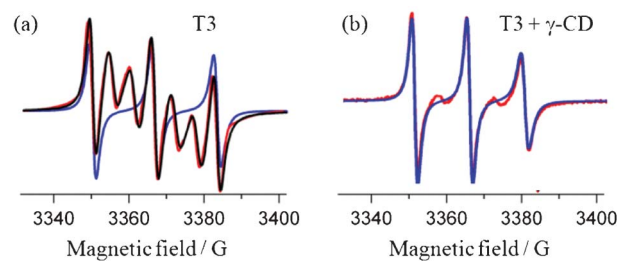


**Fig. 2** Experimental EPR spectra (black line) and their simulations (red line: addition of Lorentzian lines; blue line: computation of the three-line component) for (a) T3 in 1 : 1 MeOH-water mixture,  $A_N = 16.5$  G,  $\tau = 0.08$  ns, seven-line component = 57%; (b) T3 :  $\gamma$ -CD = 1 : 20,  $A_N = 16.6$  G,  $\tau = 0.25$  ns, five-line component = 5% [guest] = 0.1 mM;  $T = 293$  K.

spin probe which measures the guest environmental microviscosity, a reflection of the guest-host interactions.

For the EPR analysis, the spectrum of T2 in MeOH-water (Fig. 1a) was considered to be constituted of two components: (i) a multiplet of five lines at relative intensities 1 : 2 : 3 : 2 : 1 which arises from the strong electron-electron spin-spin coupling between the two nitroxide units in T2 ( $J > A_N$ ). As described in the literature,<sup>7-15</sup> this conformation may be indicated as the “close” conformation because it is assumed to arise from the close contact between the nitroxide units; and (ii) a three-line component which arises from a conformer exhibiting weak ( $J \sim 0$ ) coupling between the nitroxide units, because the two nitroxide units are in a conformation far apart (conveniently termed the “far” conformation, Scheme 2). Interconversion between the “far” and “close” conformations is considered to be responsible for the relative intensity variations among the two spectral components (three-line and five-line) and their hyperfine lines. Following the procedure explained in our earlier studies,<sup>4</sup> the binonitroxide EPR spectrum was simulated by adding the three-line computed component and a two-line component (two Lorentzian lines in between the three lines) at the proper relative intensities. The latter two-line signal was considered to belong to the five-line signal (at 1 : 2 : 3 : 2 : 1 relative intensities) expected for very strong exchange interactions. The percentage of the five-line signal was calculated with respect to the overall spectral intensity

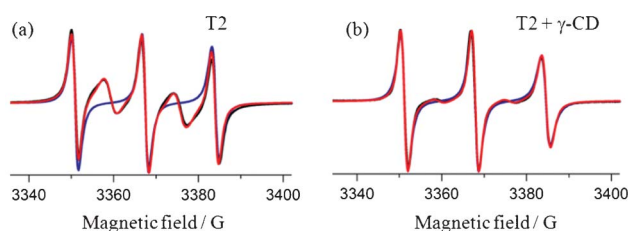
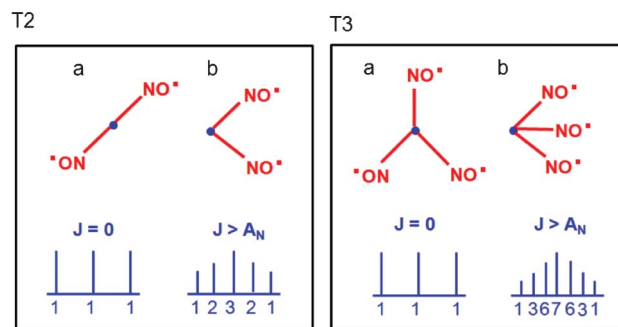


**Fig. 1** Experimental EPR spectra (black line) and their simulations (red line: addition of Lorentzian lines; blue line: computation of the three-line component) for (a) T2 in 1 : 1 MeOH-water mixture,  $A_N = 16.5$  G,  $\tau = 0.08$  ns, five-line component = 40% and (b) T2 :  $\gamma$ -CD = 1 : 20,  $A_N = 16.5$  G,  $\tau = 0.23$  ns, five-line component = 7.5%; [guest] = 0.1 mM;  $T = 293$  K.



**Scheme 2** Schematic representation of the “far” conformation (a) and the “close” conformation (b) of a binonitroxide (T2) and a trinitroxide (T3)

obtained by double integration of the experimental spectra. The proportion of the five-line exchange component of T2 in 1 : 1 MeOH–water was 40%, indicating that there was a slow exchange between the two conformers. The hyperfine coupling constant obtained from the computation of the three-line signal for T2 in MeOH–water (16.5 G) was slightly lower than that in water (17 G). The computation provided a correlation time ( $\tau$ ) of 0.08 ns, which was characteristic of fast rotating nitroxide radicals.

With the increasing addition of  $\gamma$ -CD to a solution of T2 in MeOH–water, the five-line component progressively reduced and the relative intensity of the three-line signal increased (Fig. S1 in ESI†). This effect indicates that the inclusion of at least one nitroxyl moiety of T2 within the cavity of  $\gamma$ -CD forbids the spin–spin exchange between the two nitroxide units. The experimental and simulated EPR spectra of T2 at a molar ratio host/guest = 20 : 1 ( $T = 293$  K) is shown in Fig. 1b. The exchange interaction decreases from 40% (without  $\gamma$ -CD) to 7.5% upon addition of 20 equiv. of host (Fig. 3a and Fig. S1 in ESI†). The necessity of excess host most likely is due to the low binding constant between  $\gamma$ -CD and T2. The decrease in mobility of the nitroxide with the increase of the  $\gamma$ -CD content is shown in Fig. 4a. The mobility significantly decreases ( $\tau$  increases from 0.08 to 0.16 ns) as the molar ratio increases from 0 to 5 but then it slowly decreases further at the higher molar ratios ( $\tau = 0.18$  ns at  $\gamma$ -CD/T2 = 20). The increase in  $\tau$  also supports the inclusion of the nitroxyl part of T2 within the  $\gamma$ -CD cage. No considerable change in  $A_N$  (a reflection of the environmental polarity around nitroxide) was observed from the absence (16.5 G) to the presence (16.6 G) of the host suggesting that the nitroxide groups are still exposed to the aqueous environment even upon inclusion within  $\gamma$ -CD. From our experimental data we can not conclude whether both or only one nitroxyl moiety of T2 is included within the cage to turn off the spin–spin interaction. Attempts to characterize the host–guest complexes by  $^1\text{H}$  NMR spectroscopy failed due to severe line broadening caused by the paramagnetic nitroxide.

In the absence of  $\gamma$ -CD, the experimental spectrum of T3 in water–methanol (Fig. 2a) is constituted by the superposition of the three-line component and a seven-line component, arising from the strong exchange coupling among the three nitroxide units of T3. The computation of the seven-line component was

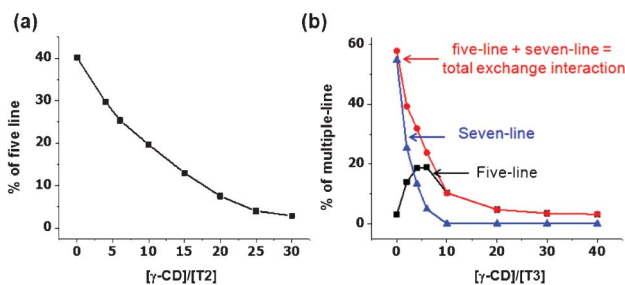


**Fig. 3** Plot for (a) the percentage of five-line component of T2 vs molar ratio of  $\gamma$ -CD : T2 and (b) the percentage of multiple-line component of T3 vs molar ratio of  $\gamma$ -CD : T3; [guest] = 0.1 mM.

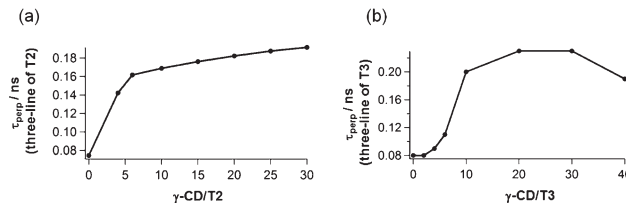
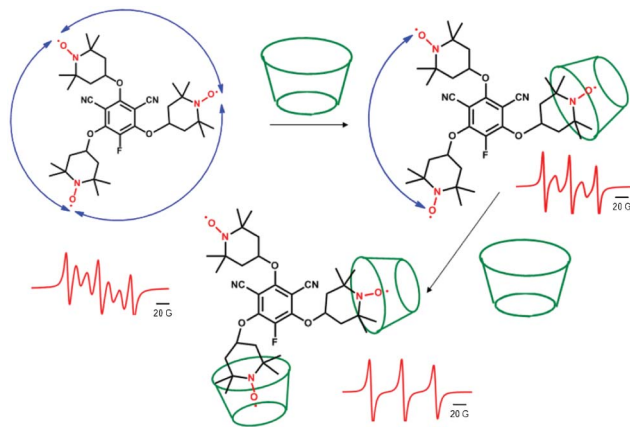


**Fig. 4** Plot for  $\tau_{\text{perp}}$  of three-line component of (a) T2 vs molar ratio of  $\gamma$ -CD : T2 and (b) T3 vs molar ratio of  $\gamma$ -CD : T3; [T2] = [T3] = 0.1 mM.

conveniently performed by adding Lorentzian lines, otherwise, as described previously,<sup>4</sup> the relative intensities of the lines could not be reproduced by considering the coupling of the electron spin with three equivalent nitrogens. The relative percentage of the seven-line component ( $J > A_N$ ) with respect to the three-line component ( $J \sim 0$ ) was 57%. It should be noted that the presence of the third nitroxide unit promotes the exchange interaction (57% for T3 vs 40% for T2). The mobility ( $\tau = 0.08$  ns) and polarity ( $A_N = 16.5$  G) of T3 (Fig. 2a), calculated for the three-line component, was the same as for T2 in solution (Fig. 1a).

We like to point out that the computation of the spectra of T2 and T3 in Fig. 1a and Fig. 2a, respectively, also needed an additional broad signal (computed as a single Lorentzian line with width of 18 G). This is probably due to a fraction (15% for T2 and 35% for T3) of undissolved T2 and T3, arising from self-aggregation of the low-polar polynitroxides in polar solvent.<sup>4</sup> Upon addition of  $\gamma$ -CD to solutions of T2 and T3 in 1 : 1 MeOH–water, the broad component of the EPR spectrum disappeared suggesting that  $\gamma$ -CD enhanced the solubility of the polynitroxides. Interestingly, the initial seven-line spectrum of T3 in the absence of  $\gamma$ -CD progressively transformed into a five-line spectrum with the addition of  $\gamma$ -CD, which further transformed into a three-line spectrum upon the addition of a large excess of  $\gamma$ -CD (Fig. S2, ESI†). This observation can be rationalized by the stepwise encapsulation of at least two of the three nitroxide units of T3 into  $\gamma$ -CD as shown in Scheme 3. The five-line component is assigned to T3 where one of the three nitroxide units is encapsulated into  $\gamma$ -CD preventing its participation in spin–spin coupling. The two remaining nitroxide units, when in a close conformation, generate the five-line spectrum. The graph for the variation of the percentage of the multiplet components versus  $\gamma$ -CD/T3 molar ratio in Fig. 3b shows the gradual transformation of the seven-line to five-line and then to three-line spectra. The highest percentage of the five-line component is observed at a  $\gamma$ -CD/T3 ratio of 5. With further addition of  $\gamma$ -CD, the equilibrium shifted to two nitroxide units of T3 being encapsulated within  $\gamma$ -CD and one remaining free. In this case a three-line spectrum is observed because no spin–spin coupling is possible. At this point we cannot exclude the possibility of all three nitroxide units being encapsulated within  $\gamma$ -CD.

It is interesting to follow the variation of the correlation time for motion for the three-line component as a function of



**Scheme 3** Schematic representation of the stepwise encapsulation of T3 with  $\gamma$ -CD and observed EPR spectra (red).

the molar ratio between  $\gamma$ -CD and T3 (Fig. 4b) and  $\gamma$ -CD and T2 (Fig. 4a). The point at which the mobility starts decreasing provides a measure of the starting point of the inclusion of the second nitroxide unit into the  $\gamma$ -CD cage.

Our next set of experiments were aimed at measuring the thermodynamic parameters ( $\Delta H$  and  $\Delta S$ ) for the exchange between the “far” and “close” conformers of polynitroxides, in the absence and presence of  $\gamma$ -CD. It is reported that the logarithmic (Arrhenius) plot of the lifetime ratio of the two conformers ( $\tau_{J>A_N}/\tau_{J\sim 0}$ , also indicated as  $t_{\text{close}}/t_{\text{far}}$  or  $t_b/t_a$ ) vs. the inverse of temperature leads to measure the above thermodynamic parameters.<sup>4,16,17</sup> EPR spectra of the polynitroxides were recorded in the absence and presence of  $\gamma$ -CD at various temperatures. Fig. 5 and Fig. S3 (ESI†) show examples of the spectra recorded at increasing temperature for T2 and T3, respectively, both in MeOH and water. Upon increasing  $T$  from 293 to 343 K, the EPR spectra of both T2 and T3 in 1 : 1 MeOH–water mixture became well resolved and the amount of broad component needed for the computation decreased, suggesting the reduction of self-aggregation of the polyradicals with temperature (Fig. 5 and Fig. S3 in ESI†).

In addition, the decrease in line width by increasing  $T$  resolved more than two lines in between the three-line component ( $J = 0$ ) for T2, as shown in Fig. 5. At higher temperatures the EPR spectrum of the nitroxide biradical consists of the three-line component (for the “far” conformation), corresponding to the nuclear configurations  $I(1) = I(2) = -1, 0, +1$ , and other six lines for the “close” conformation,

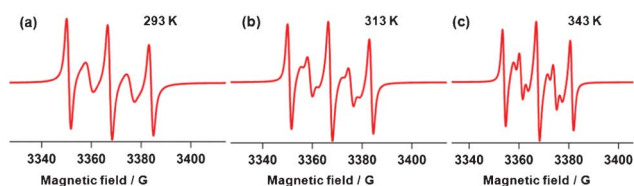


**Fig. 5** EPR spectra of T2 in 1 : 1 MeOH–water at various temperatures (a) 293, (b) 313 and (c) 343 K; [T2] = 0.1 mM.

which appear in between the three lines and correspond to the nuclear configurations  $I(1) = I(2)$  (0,1; 1,0; 1,-1; -1,1; -1,0; 0,-1). The averaged  $J$  coupling coefficient may be calculated from theory as  $J = A_N^2/(2g\beta\Delta B - 2A_N)$ , where  $\Delta B$  is the distance between the 2nd (0,1) and the 8th (0,-1) lines (Fig. 5).<sup>16–20</sup> We obtain  $J = 120$  MHz which corresponds to about  $J/A_N = 2.5$ . In our previous study on the polynitroxides in chloroform solutions,<sup>4</sup> we only obtained two lines between the three main lines instead of six because in a less polar and more fluid solvent (such as  $\text{CHCl}_3$ ) the exchange coupling is stronger and the  $J$  value could not be correctly estimated. However, as we note from Fig. 5, the positions of the lines did not change by increasing temperature and this is in line with a slow exchange between the “far” and the “close” conformers which is a necessary condition to calculate the thermodynamic parameters.

The relative intensities of the lines of the multiplets arising from the spin–spin exchange interaction between the nitroxide units in “close” conformation, and the three lines (from nitroxide units in “far” conformation) at variable temperatures were used to estimate the thermodynamic parameters, such as  $\Delta H$  and  $\Delta S$ . These calculations have been described in detail previously.<sup>4</sup> Briefly, the EPR line intensity ratios between the multiplet of lines and the three lines was considered proportional to the ratio of the time spent in the “close” conformation ( $\tau_{J>A_N}$ ) and the “far” conformation ( $\tau_{J\sim 0}$ ). The logarithmic plot of this ratio ( $t_{\text{close}}/t_{\text{far}}$ ) vs. the inverse temperature is an Arrhenius plot (Fig. 6) monitoring the kinetics of the conformation change.  $\Delta H$  is extracted from the slope of this plot ( $-\Delta H/R$ ) and  $\Delta S$  is determined from the intercept ( $\Delta S/R$ ). Fig. 6, Fig. S4 (ESI†) and S5 (ESI†) display the Arrhenius plots for T2 and T3 in the absence and presence of  $\gamma$ -CD and the extracted thermodynamic parameters are summarized in Table 1. We selected the  $\gamma$ -CD/polynitroxide ratio to be 20 because, at this ratio, the EPR analysis, as described above, indicated the thermodynamically stable inclusion of the nitroxides into the  $\gamma$ -CD cage.

To interpret these data, we have to consider that, from a thermodynamic point of view, an increase in  $\Delta H$  reflects the increased energy needed for the nitroxides to approach each other, whereas an increase in  $\Delta S$  reflects the increased complexity of the system. By comparing the thermodynamic parameters of T2 in the absence and presence of  $\gamma$ -CD, it is

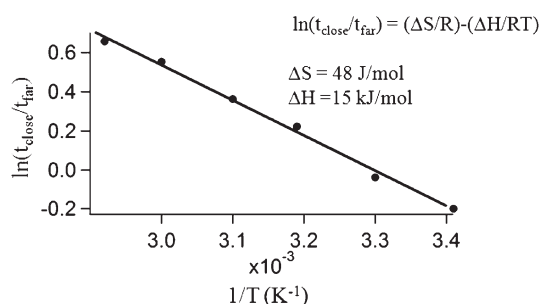


**Fig. 6** Arrhenius plot for T2 in 1 : 1 MeOH–water.

**Table 1** The parameters extracted from the EPR spectra of the probes in the absence and presence of  $\gamma$ -CD

Sample	$A_N$ (G)	$\tau$ (ns)	Exchange component	$\Delta H$ (kJ mol <sup>-1</sup> )	$\Delta S$ (J K <sup>-1</sup> mol <sup>-1</sup> )
T2	16.5	0.08	five-line = 40%	15	48
T2/ $\gamma$ -CD = 1 : 20	16.5	0.23	five-line = 7.5%	45	121
T3	16.5	0.08	seven-line = 57%	19	69
T3/ $\gamma$ -CD = 1 : 20	16.6	0.25	seven-line = 0%, five-line = 5%	14	42

found that both the enthalpy and the entropy of the transition process increase from the absence to the presence of  $\gamma$ -CD (Table 1). This increase can be rationalized with the additional step of decomplexation of the nitroxide from  $\gamma$ -CD, which is necessary before spin exchange coupling can occur between the two nitroxides in the presence of  $\gamma$ -CD. According to EPR analysis, at higher temperatures, the equilibrium between  $\gamma$ -CD complexed nitroxides and free nitroxides is shifted to free nitroxides, which promotes spin–spin exchange. Direct comparison of the thermodynamic parameters for T3 in the absence and presence of  $\gamma$ -CD is more complex. In the absence of  $\gamma$ -CD, T3 shows temperature dependent EPR spectra characteristic for spin coupling in a three-spin system. However, in the presence of a 20-fold excess of  $\gamma$ -CD, T3 shows EPR spectra characteristics for spin coupling in a two-spin system throughout the investigated temperature range. The observation of the two-spin system can be rationalized that at any given time at least one of the nitroxides is complexed by  $\gamma$ -CD. Therefore, changes in the thermodynamic parameters (Table 1) in the presence of  $\gamma$ -CD are probably dominated by the change from the three-spin to the two-spin system.

## Conclusions

Spin interactions between the nitroxide units of polynitroxides can be quenched by inclusion of the nitroxide moiety within a host such as  $\gamma$ -CD. Variation of the host/guest ratio tunes the nature of a trinitroxide spin system from a three-spin to a two-spin to a one-spin system. Given the role of nitroxyl polyradicals for use in dynamic nuclear polarization (DNP), controlling their spin–spin interactions through supramolecular assemblies as described here could play a significant role in the development of a more sensitive and tunable DNP. Furthermore, these polynitroxides were revealed to be good probes to follow the encapsulation and interacting ability of cages like CD which are biologically relevant as drug carriers.

## Acknowledgements

VR and NJT thank the National Science Foundation, USA for generous financial support through grants CHE-0848017 and CHE-1111398, respectively.

## References

- 1 K. Sze, Q. Wu, H. Tse and G. Zhu, *NMR of Proteins and Small Biomolecules*, ed. G. Zhu, Springer, Berlin/Heidelberg, 2012, vol. 326, pp. 215–242.
- 2 Y. Matsuki, T. Maly, O. Ouari, H. Karoui, F. Le Moigne, E. Rizzato, S. Lyubenova, J. Herzfeld, T. Prisner, P. Tordo and R. G. Griffin, *Angew. Chem., Int. Ed.*, 2009, **48**, 4996–5000.
- 3 M. Porel, M. F. Ottaviani, S. Jockusch, N. Jayaraj, N. J. Turro and V. Ramamurthy, *Chem. Commun.*, 2010, **46**, 7736–7738.
- 4 M. F. Ottaviani, A. Modelli, O. Zeika, S. Jockusch, A. Moscatelli and N. J. Turro, *J. Phys. Chem. A*, 2011, **116**, 174–184.
- 5 O. Zeika, Y. Li, S. Jockusch, G. Parkin, A. Sattler, W. Sattler and N. J. Turro, *Org. Lett.*, 2010, **12**, 3696–3699.
- 6 D. E. Budil, S. Lee, S. Saxena and J. H. Freed, *J. Magn. Reson., Ser. A*, 1996, **120**, 155–189.
- 7 J. Fritscher, M. Beyer and O. Schiemann, *Chem. Phys. Lett.*, 2002, **364**, 393–401.
- 8 S. J. Jacobs, D. A. Shultz, R. Jain, J. Novak and D. A. Dougherty, *J. Am. Chem. Soc.*, 1993, **115**, 1744–1753.
- 9 A. Kokorin, V. Tran, K. Rasmussen and G. Grampp, *Appl. Magn. Reson.*, 2006, **30**, 35–42.
- 10 A. Rajca, S. Mukherjee, M. Pink and S. Rajca, *J. Am. Chem. Soc.*, 2006, **128**, 13497–13507.
- 11 H. Sato, V. Kathirvelu, G. Spagnol, S. Rajca, A. Rajca, S. Eaton and G. R. Eaton, *J. Phys. Chem. B*, 2008, **112**, 2818–2828.
- 12 D. A. Shultz, S. H. Bodnar, H. Lee, J. W. Kampf, C. D. Incarvito and A. L. Rheingold, *J. Am. Chem. Soc.*, 2002, **124**, 10054–10061.
- 13 D. A. Shultz, R. M. Fico, S. H. Bodnar, R. K. Kumar, K. E. Vostrikova, J. W. Kampf and P. D. Boyle, *J. Am. Chem. Soc.*, 2003, **125**, 11761–11771.
- 14 V. A. Tran, K. Rasmussen, G. Grampp and A. I. Kokorin, *Appl. Magn. Reson.*, 2007, **32**, 395–406.
- 15 R. West, J. D. Cavalieri, J. J. Buffy, C. Fry, K. W. Zilm, J. C. Duchamp, M. Kira, T. Iwamoto, T. Müller and Y. Apeloig, *J. Am. Chem. Soc.*, 1997, **119**, 4972–4976.
- 16 V. N. Parmon, A. I. Kokorin, G. M. Zhidomirov and K. I. Zamaraev, *Mol. Phys.*, 1973, **26**, 1565–1569.
- 17 V. N. Parmon, A. I. Kokorin, G. M. Zhidomirov and K. I. Zamaraev, *Mol. Phys.*, 1975, **30**, 695–701.
- 18 J. Szydłowska, K. Pietrasik, Ł. Gład and A. Kaim, *Chem. Phys. Lett.*, 2008, **460**, 245–252.
- 19 G. R. Luckhurst, *Mol. Phys.*, 1966, **10**, 543–550.
- 20 G. R. Luckhurst and G. F. Pedulli, *Mol. Phys.*, 1970, **18**, 425–428.